Chemical Science

ROYAL SOCIETY OF CHEMISTRY

EDGE ARTICLE

View Article Online
View Journal

Cite this: DOI: 10.1039/d2sc05735b

All publication charges for this article have been paid for by the Royal Society of Chemistry

Benzoates as photosensitization catalysts and auxiliaries in efficient, practical, light-powered direct C(sp^3)–H fluorinations†

Shahboz Yakubov, [a] Willibald J. Stockerl, [a] Xianhai Tian,[a] Ahmed Shahin, [ab] Mark John P. Mandigma, [a] Ruth M. Gschwind [a] and Joshua P. Barham [*a]

Of the methods for direct fluorination of unactivated C(sp^3)–H bonds, photosensitization of SelectFluor is a promising approach. Although many substrates can be activated with photosensitizing catalysts, issues remain that hamper fluorination of complex molecules. Alcohol- or amine-containing functional groups are not tolerated, fluorination regioselectivity follows factors endogenous to the substrate and cannot be influenced by the catalyst, and reactions are highly air-sensitive. We report that benzoyl groups serve as highly efficient photosensitizers which, in combination with SelectFluor, enable visible light-powered direct fluorination of unactivated C(sp^3)–H bonds. Compared to previous photosensitizer architectures, the benzoyls have versatility to function both (i) as a photosensitizing catalyst for simple substrate fluorinations and (ii) as photosensitizing auxiliaries for complex molecule fluorinations that are easily installed and removed without compromising yield. Our auxiliary approach (i) substantially decreases the reaction's induction period, (ii) enables C(sp^3)–H fluorination of many substrates that fail under catalytic conditions, (iii) increases kinetic reproducibility, and (iv) promotes reactions to higher yields, in shorter times, on multigram scales, and even *under air*. Observations and mechanistic studies suggest an intimate 'assembly' of auxiliary and SelectFluor prior/after photoexcitation. The auxiliary allows other E_nT photochemistry *under air*. Examples show how auxiliary placement proximally directs regioselectivity, where previous methods are substrate-directed.

Received 15th October 2022
Accepted 28th October 2022

DOI: 10.1039/d2sc05735b

rsc.li/chemical-science

Introduction

Although numerous methods have been developed for fluorination reactions of C–H bonds, such as the fluorination of carbanions,[1] arylpalladium complexes,[2] and the addition of electrophilic fluorine to alkenes,[3] few methods permit the direct fluorination of unactivated C(sp^3)–H bonds.[4] Such a transformation is particularly advantageous for the late-stage functionalization (LSF) of complex molecules. Especially, since F atoms as H atom bioisosteres impart vastly different – and usually favorable – properties (physical, ADME, lipophilicity) in a pharmaceutical/agrochemical context.[5] Of these, methods that involve photosensitization of SelectFluor (**SF**) are particularly attractive for their mild conditions and use of light as a sustainable, uncontaminating energy source to drive reactivity.[6] Here, **SF** functions as both a fluorine source and an activator of C(sp^3)–H bonds; since quinuclidinium-type radical cations are powerful and selective hydrogen atom transfer (HAT) agents.[7] Pioneering studies by Chen[8] and Tan[9] demonstrated photocatalytic, direct fluorinations of unactivated C(sp^3)–H bonds by employing acetophenone or anthraquinone (**AQN**) as photosensitization catalysts (**PSCat**s, Fig. 1A). Fluorination regioselectivity was governed by thermodynamic factors endogenous to the substrate; the most electron-rich C(sp^3)–H bond that forms a stable 2° radical intermediate is fluorinated. Lectka used benzil as an alternative **PSCat** for the late-stage photocatalytic fluorination of complex molecules,[10] including steroid derivatives, and found that ketones/enones innate to the substrate could direct regioselective C(sp^3)–H fluorination in a proximal or distal fashion (Fig. 1A). Further examples of photosensitized C(sp^3)–H fluorination have successfully engaged benzylic positions of simple substrates[10a] or complex peptides,[10c] as well as ketal substrates.[10e]

In most cases, **PSCat**s belonged to the family of aryl ketones as a privileged architecture for photosensitization, whose success has been attributed to the matching of triplet energies with **SF**.[9a] While the utilized aryl ketone catalysts alone do not absorb visible light, their assembly with **SF** affords a charge transfer complex with a tailing absorption >400 nm.[9b] However, in all cases fluorinations of molecules containing 1°/2° alcohols or amines were unsuccessful (only 3° alcohols were tolerated),

[a]*Fakultät für Chemie und Pharmazie, Universität Regensburg, 93040 Regensburg, Germany. E-mail: Joshua-Philip.Barham@chemie.uni-regensburg.de*

[b]*Chemistry Department, Faculty of Science, Benha University, 13518 Benha, Egypt*

† Electronic supplementary information (ESI) available. CCDC 2212436 and 2212438. For ESI and crystallographic data in CIF or other electronic format see DOI: https://doi.org/10.1039/d2sc05735b

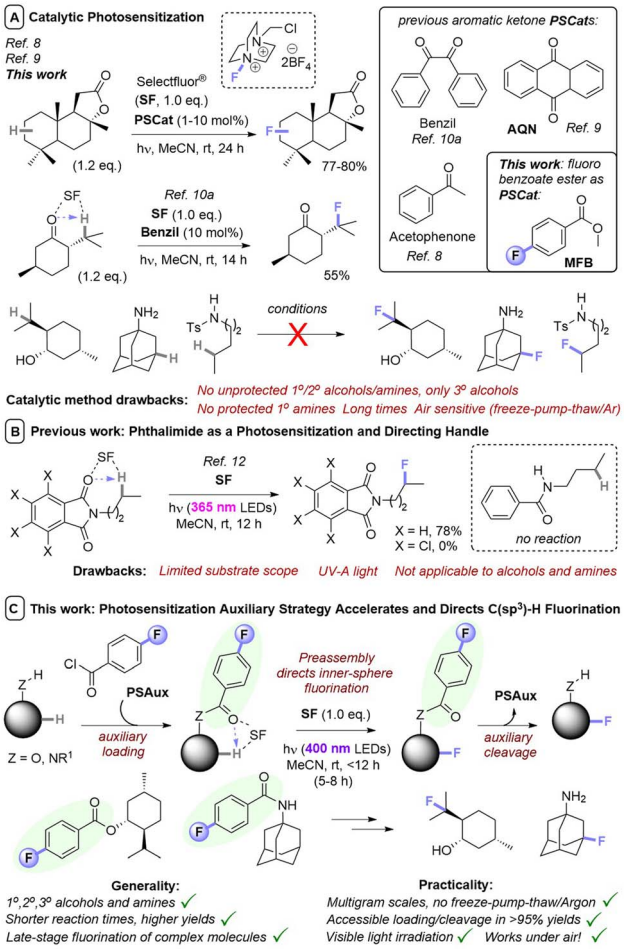

Fig. 1 Photochemical direct fluorination of unactivated C(sp^3)–H bonds. (A) Previous uses of catalytic aryl ketone photosensitizers and discovery herein of a catalytic benzoate photosensitizer. (B) Phthalimides as a photosensitization handle. (C) A general, efficient, selective, and rapid photosensitization auxiliary strategy using benzoyl groups.

likely due to competing nucleophilic destruction of **SF** when the photochemical reaction is kinetically slow.[11] This severely hampers applications to complex bioactive molecules such as pharmaceuticals. Recently, Egami and Hamashima[12] found molecules with *N*-alkylphthalimides underwent directed photochemical C(sp^3)–H fluorination of their alkyl chains (Fig. 1B). However, both an *N*-alkyl tetrachlorophthalimide and an *N*-alkyl benzamide derivative were unsuccessful, leading authors to suggest a key role for the phthalimide's triplet energy. The phthalimide could be considered as a 'photosensitization auxiliary' (**PSAux**) that can be cleaved to reveal a fluorinated 1° amine, though this was not realized and would typically require toxic, explosive hydrazine.

We envisioned a **PSAux** that is easily incorporated and removed could increase the generality and rapidity of photochemical C(sp^3)–H fluorinations. The **PSAux** may form an intimate assembly with **SF** for inner-sphere photochemistry, increasing reaction efficiency. Moreover, an appropriately designed **PSAux** (*e.g.* containing a C=O group[10a]) may even provide an exogenous user handle to direct regioselectivity for the first time, where all previous reports follow factors/functionality endogenous to the substrate. Herein, we report the discovery of benzoyl groups as novel, versatile photosensitizer architectures. Methyl 4-fluorobenzoate serves as a photosensitizing catalyst for fluorination of simple substrates, while the 4-fluorobenzoyl group serves as a **PSAux** for the fluorination of complex molecules containing alcohols and amines and can be easily installed and removed without compromising product yields. The **PSAux** strategy (i) markedly increases the efficiency, rapidity, reliability and practicality of C(sp^3)–H fluorination reactions; (ii) enables reactions of substrates that cannot be engaged with photocatalysis (alcohols and amines, where previous catalytic methods were generally only applicable to 3° alcohols); (iii) allows reactions to succeed under air atmosphere and (iv) offers promise to direct fluorination regioselectivity (Fig. 1C).

Results and discussion

Discovery

When examining the C(sp^3)–H fluorination of amyl benzoate **1a** to **2a** as reported by Tan and co-workers[9a] (Table 1, entries 1 and

Table 1 Initial investigations and optimization of conditions[a]

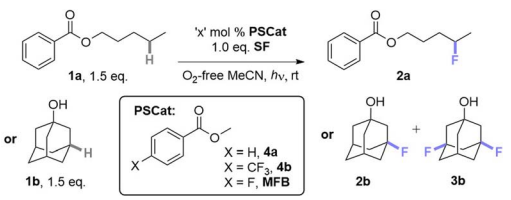

Entry	Substrate[b]	PSCat, 'x'	λ (nm)	*t* (h)	Product, yield[c]
1	**1a**	**AQN**, 2%	365	48	**2a**, 46%
2	**1a**	**AQN**, 2%	400	48	**2a**, 46%
3	**1a**	—	365	48	**2a**, 55%
4	**1a**	—	400	48	**2a**, 44%
5	**1a**	—	451	24	**2a**, n.d.
6	**1a**	—	—	24	**2a**, n.d.
7	**1b**	**1a**, 5%	400	24	**2b**, <5%; **3b**, n.d.
8	**1b**	**4a**, 5%	400	24	**2b**, n.d.; **3b**, n.d.
9	**1b**	**4b**, 5%	400	24	**2b**, <5%; **3b**, n.d.
10	**1b**	**MFB**, 5%	400	24	**2b**, 43%; **3b**, 3%
11	**1b**	—	400	48	**2b**, <5%; **3b**, n.d.
12	**1b**	**MFB**, 5%	400	48	**2b**, 53%; **3b**, 5%
13	**1b**	**MFB**, 10%	400	48	**2b**, 65%; **3b**, 6%
14[d,e]	**1b**	**MFB**, 10%	400	24	**2b**, 75%; **3b**, 6%
15	**1b** [0.31 M]	**MFB**, 1%	400	48	**2b**, 60%; **3b**, 12%
16[d]	**1b** [0.31 M]	**MFB**, 1%	400	6	**2b**, 28%; **3b**, 3%
17[d,f]	**1b** [0.31 M]	**MFB**, 1%	400	24	**2b**, 84%; **3b**, 10%
18[g]	**1b** [0.31 M]	**MFB**, 1%	400	24	**2b**, <5%; **3b**, n.d.

[a] nd., not detected. [b] Unless otherwise specified, substrate concentration was [0.16 M] and a 0.35 W (input) 400 nm LED was employed. [c] Yields determined by ^{19}F NMR spectroscopy with trifluorotoluene as an internal standard and correspond to combined fluorinated regioisomers. [d] A 3.8 W (input) LED was employed. [e] Hereafter termed conditions **A**. [f] Hereafter termed conditions **B**. [g] Prepared under air.

2) with **AQN** and derivatives, we found that no catalyst was necessary; the reaction proceeded in its absence at 365 and 400 nm (entries 3 and 4). The **PSCat**-free reaction did not proceed at 451 nm or in the absence of light (entries 5 and 6). Assuming that **1a** was acting as a photosensitizer for its own self-fluorination, we reasoned that arylbenzoate esters may function as exogenous **PSCat**s in the C(sp^3)–H fluorination of 1-adamantanol **1b** to **2b** and **3b**. However, **1a** was an ineffective **PSCat** (entry 7). Assuming that self-fluorination of **1a** may deactivate its catalysis of the fluorination of **1b**, methyl benzoate (**4a**) was attempted but was similarly unsuccessful (entry 8).

While other *para*-substituted benzoate esters (**4**, where X = Cl, Br or CF_3, entry 9) were also ineffective (also see ESI†), methyl 4-fluorobenzoate (**MFB**) was a surprisingly effective **PSCat** (entry 10), delivering a 46% yield of **2b**(**+3b**) compared to an ineffective control reaction without **PSCat** (entry 11). Employing 10 mol% of **MFB** provided **2b+3b** in an improved 71% yield (entry 13). Doubling the overall concentration of **1b** to 0.31 M and decreasing catalyst loading at this higher overall concentration also improved the yield (entry 15). For both the low and high concentration conditions, a higher power LED further increased the yield of **2b+3b** in a shorter reaction time (entries 14 and 17, termed 'conditions **A**' and 'conditions **B**', respectively), although 6 h was here insufficient for full conversion (entry 16). Air, protic additives and using an equimolar ratio of SelectFluor (*vs.* substrate) were all detrimental to the reaction (for full investigations, see ESI†).

Synthetic scope of PSCat method

Under these photocatalytic conditions, the C(sp^3)–H fluorinations of a variety of small molecules was achieved in modest to excellent (31–94%) yields (Table 2). Though electronically bearing resemblance to amyl benzoate, substrates **1c–1e** did not fluorinate in the absence of **MFB**. Substrates **1d–1g** underwent fluorination not at their benzylic nor terminal positions but at the most electron-rich C(sp^3)–H bond that involves a 2° radical intermediate. Substrates **1h–1j** underwent benzylic fluorination likely due to their benzylic C(sp^3)–H bonds being the least electron-deficient. Aliphatic esters **1k**, **1l** (sclareolide), **1y** (ibuprofen methyl ester) – and aliphatic ketone **1m** – were all fluorinated at their most electron-rich (or benzylic) C(sp^3)–H bonds remote from the carbonyl group. Steroidal derivatives **1o**, cholest-4-en-3-one (**1p**) were successfully fluorinated. Bromoalkane **1q**, cyanoalkane **1r** and trialkylamine **1s** were fluorinated at their most electron rich C(sp^3)–H positions. When unactivated hydrocarbons **1t–1x** were subjected to the reaction, C(sp^3)–H fluorination was selective for 3° positions > 2° positions (when present). Both pyrrolidinium and imidazolium-type ionic liquids (**1aa**, **1ac–1ae**) and a common food flavor additive (undecanoic γ-lactone, **1ab**) were fluorinated in good to excellent (61–99%) yields demonstrating (i) the tolerance of heterocyclic motifs (also see **1l**) and (ii) synthetic utility of the method for 'real-world' molecules.

Despite a reasonably broad scope of applications of this catalytic method, we noticed that apart from 3° alcohols (*e.g.* **1b**), free alcohols (**5a**, **5b′**, **5c–5e**, **5g**) and free amines (**6a–6d**) all failed under photocatalytic C(sp^3)–H fluorinations (Table 3). We note that in the earlier reports of Chen,[8] Tan,[9a] and Lectka,[10a–e] free 1° or 2° alcohols were never reported, only hindered 3° alcohols were tolerated. Neither were free 1°/2°/3° amine moieties; 1° and 2° amines always required protection. Even protected 1° amide **7** did not fluorinate in this case. One explanation could be that if the desired reactivity is too slow, nucleophilic destruction of SelectFluor (known to occur with 1° and 3° amines)[13] may emerge as a competitive thermal reaction, arising lower yields or no reactivity. The steric hindrance of 3° alcohols – the only class of free alcohols that worked in the previous reports – may explain their tolerance. However, since nucleophilic 3° amines did proceed (**1s**, **1z**) albeit in low (33%, 18%) yields, there may be other factors responsible for the failure of 1° and 2° alcohols/amines/amides. **SF**'s known interactions with a wide range of functional groups in ground state chemistry – such as Lewis acid interactions with C–O bonds and fluorinations of nucleophilic (S,N) atoms[14] – are likely detrimental to its use in photocatalytic C(sp^3)–H fluorinations. Another explanation is that hydrogen bonding networks around alcohol/water-solvated **SF** prohibit its non-covalent assembly with the aromatic **PSCat** that is needed for successful photochemistry (*vide infra*).[9b] Interestingly, although **5b** has no unprotected alcohol and contained a privileged benzylic C(sp^3)–H bond, it also reacted poorly (8% yield).

Synthetic scope of PSAux method

At this juncture, we considered that a key advantage of our 4-fluorobenzoate photosensitizer compared to previously-employed aryl ketone **PSCat**s was the ability to reversibly attach it to alcohol and amine substrates and then detach it after photochemical fluorination (both under simple conditions): a 'photosensitization auxiliary' (**PSAux**) approach.

Not only would this enable C(sp^3)–H fluorinations that were catalytically inefficient or impossible (such as complex molecules), it would accelerate reaction kinetics and improve reproducibility (*vide infra*). Moreover, it would improve practicality by decreasing atmospheric sensitivity and simplify purification of otherwise highly polar unprotected substrates. Thus, a variety of alcohols **8** and amines **10** were loaded with the 4-fluorobenzoate **PSAux** in near-quantitative yields. To our delight, auxiliary-loaded alcohols **8a–i** all underwent C(sp^3)–H fluorination (Table 3), generally in good to excellent (57–90%) yields. Interestingly, where benzoate ester **5b** provided only 8% yield, its 4-fluorobenzoate derivative **8b** was fluorinated to afford **9b** in 75% yield, highlighting the benefit of the **PSAux** in improving efficiency (even when unprotected alcohols/amines are absent). Moreover, while the catalytic fluorination affording **2k** was completely ineffective under air, the yield of **9b** (74%) was unaffected by setting up *under air*. Although the reaction of **1a** without any catalyst gave a 44% yield of **2a** (Table 1, entry 4), however, its **PSAux** derivative, amyl 4-fluorobenzoate, led to a 78% yield of **9j** again confirming the benefit of the F atom in the **PSAux**. Though lithocholic acid derivative **8k** only afforded a 23% yield of **9k**, the C(sp^3)–H fluorination of steroid

Table 2 Scope of photocatalytic C(sp^3)–H fluorination method[a]

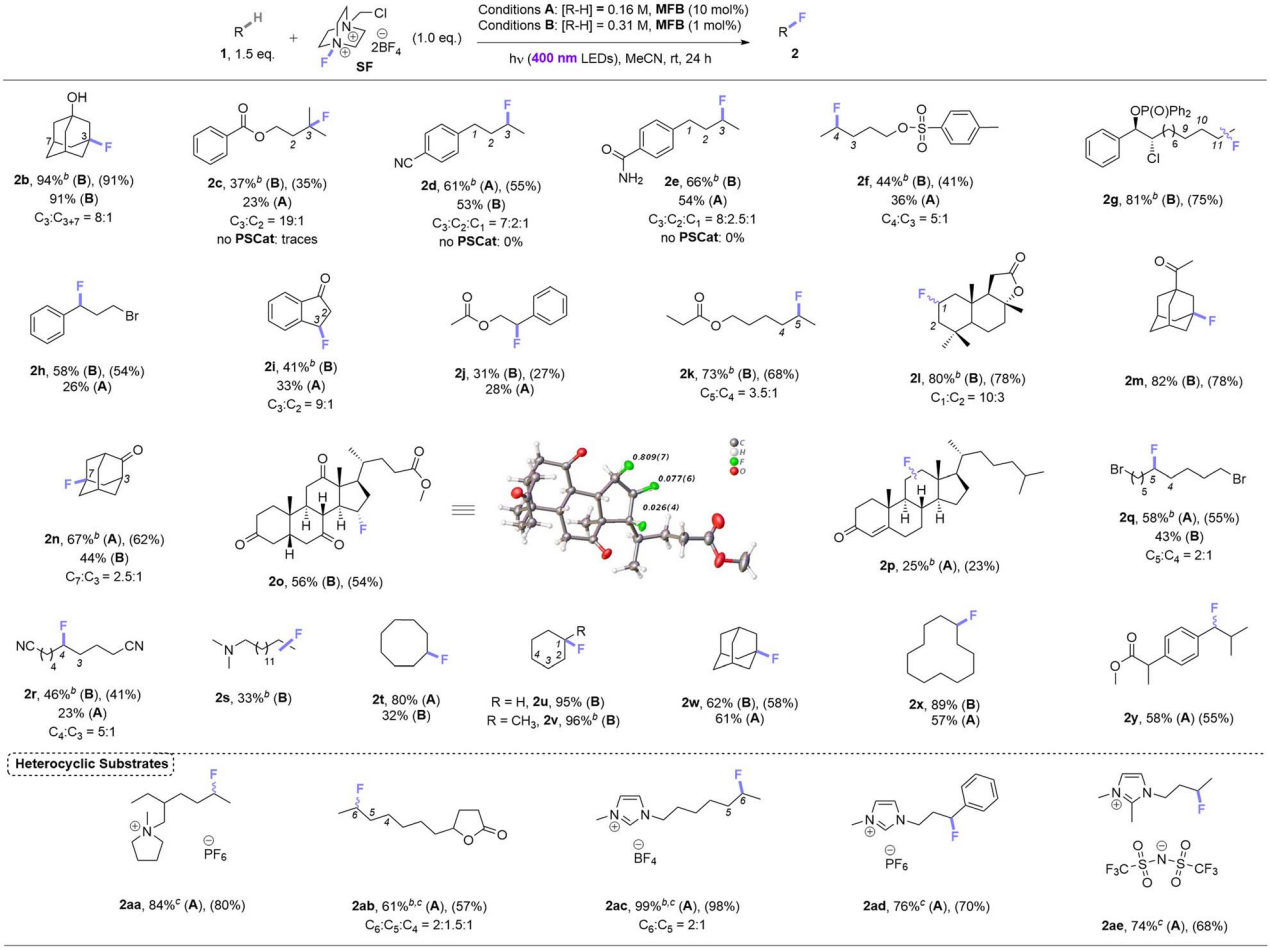

[a] For substrates with more than one regioisomer, the major isomer is depicted. NMR yields were determined by ^{19}F NMR with trifluorotoluene as internal standard (IS). Unless explicitly defined, yields correspond to a single regioisomer. Isolated yields in parenthesis. [b] Yield corresponds to the combined mixture of regioisomers. [c] 2.0 eq. of **SF** used.

derivatives was only possible previously with in-built enone/ketone/ketal protecting/directing groups.[10]

Gratifyingly, the C(sp^3)–H fluorination of amines was also enabled *via* their auxiliary-loaded amide forms **10a–10e**, affording **11a–11e** in moderate to very good (32–72%) yields. The profound increase in reactivity from having the fluorine in the 4-position of the benzoate group was apparent here. Substrate **10a** was successfully engaged, while the previously attempted photochemical fluorination of *N*-butylbenzamide (Fig. 1B)[12] gave no reaction. Although phthalimides[12] offer the potential to serve as a **PSAux**, the 4-fluorobenzoyl **PSAux** is both more effective and generally applicable since (i) phthalimides can only function in this way for 1° amines and ii) benzoates undergo straightforward deprotection (*vide infra*). To our surprise, the auxiliary loaded amide derived from Fingolimod **10f** did not require any subsequent protection of its two free 1° alcohols. In summary, incorporation of a **PSAux** accelerates the rate of C(sp^3)–H fluorination to a point that it (i) outcompetes the catalytic method, (ii) outcompetes degradation of **SF**, (iii) allows energy transfer (E_nT) photosensitization reactions to succeed *under air*. This renders the **PSAux** an attractive strategy for C(sp^3)–H fluorination of complex, bioactive molecules like active pharmaceutical ingredients, exemplified by the successful fluorination of phenylcyclohexylglycolic acid (**8i**), a derivative of lithocholic acid (**8k**), multiple sclerosis active pharmaceutical intermediate (API) Fingolimod (**10f**) and anti-diabetic API vildagliptin (**10g**).

Noticing that antipsychotic API Haloperidol **12** contains a 4-fluoroacetophenone moiety, we reasoned its photochemical C(sp^3)–H fluorination may occur without *any* catalyst or auxiliary. Indeed, its reaction successfully gave **13** in 43% yield (Fig. 2A). Haloperidol and Fingolimod feature in the top 200 pharmaceuticals by retail sales in 2020[15] and their late-stage fluorination opens avenues to new chemical space and pharmacological activities. Finally, we investigated the impact of **PSAux** location on C(sp^3)–H fluorination selectivity by the late-

Table 3 Scope of photosensitization auxiliary C(sp^3)–H fluorination method. (A) Unreactive, unprotected substrates. (B) Scope of photosensitization auxiliary method[a]

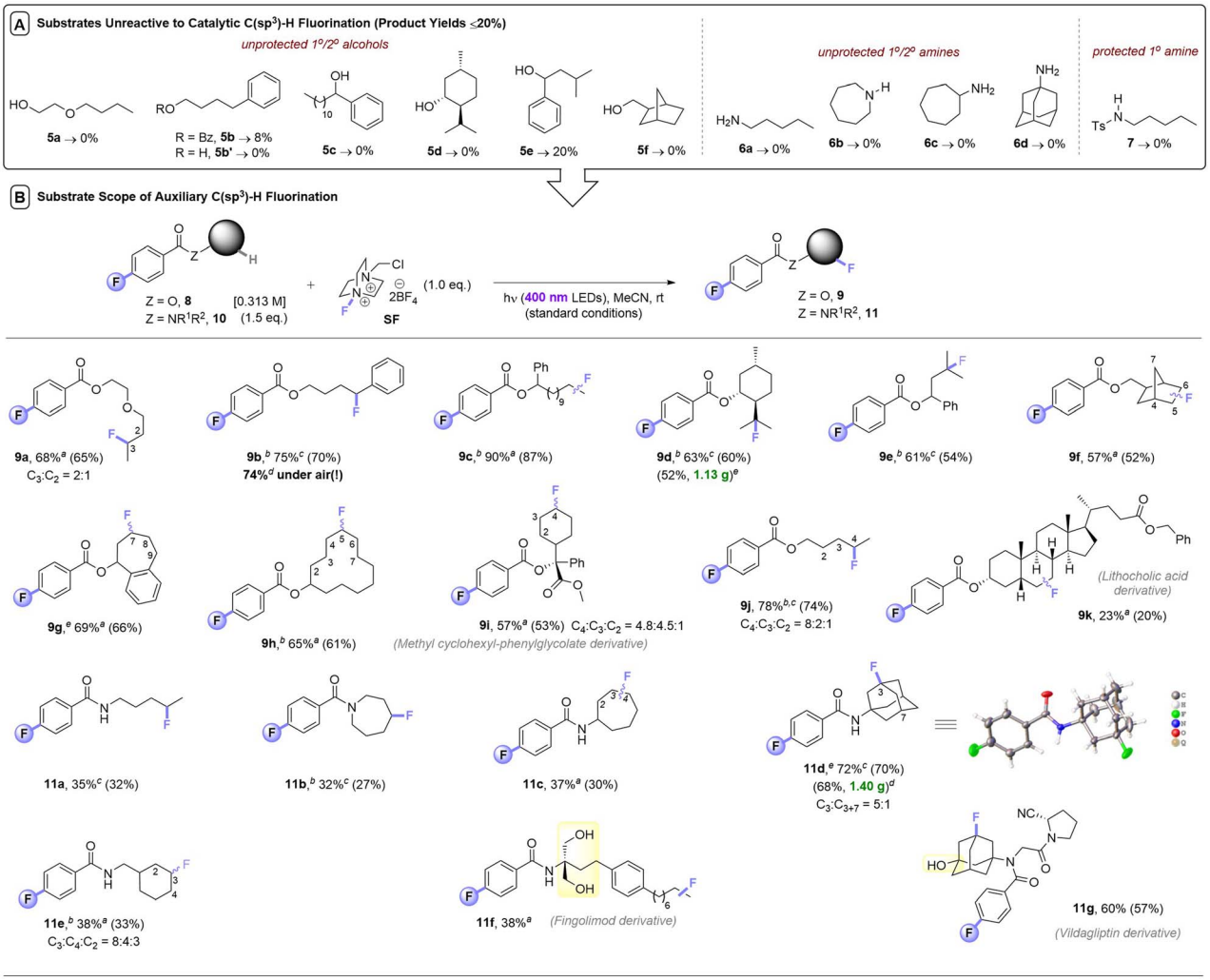

[a] For substrates with more than one regioisomer, the major isomer is depicted. NMR yields were determined by ^{19}F NMR with trifluorotoluene as internal standard (IS). Unless explicitly defined, yields correspond to a single regioisomer. Isolated yields in parenthesis. [b] Yield corresponds to a mixture of regioisomers. [c] Reaction completed in 10 h. [d] Yield corresponds to a single regioisomer. [e] Isolated yields of gram scale reactions. [f] Reaction completed in 5 h.

stage fluorination of Dextromethorphan **1z** (Fig. 2B). The photocatalytic method with **MFB** was inefficient, affording an unsatisfactory (18%) yield of **2z.** Following attachment of the **PSAux** to **1z** by tandem *N*- or *O*-demethylation/**PSAux** loading – affording **10h** and **8l** in high yields over 2 steps (85 and 87%, respectively) – their photochemical C(sp^3)–H fluorinations afforded **11h** and **9l** in satisfactory yields (42 and 48%, respectively). Interestingly, **11h** was afforded as two fluorinated regioisomers on the 'B' ring (possibly assisted by a developing fluorine gauche effect)[16] while **9l** was a single regioisomer on the 'C' ring. Therefore, our **PSAux** auxiliary strategy offers future promise as an attachable handle to direct late-stage C(sp^3)–H fluorination selectivity which (i) is not possible by previous catalytic methods and (ii) allows fluorination to be exogenously directed by the chemist, rather than endogenously directed by the molecule *via* its inherent functionality.[9a,10,12] Of key importance and justifying the use of a **PSAux** strategy, the 4-fluorobenzoate auxiliaries can be cleaved by known methods[17] to give alcohols or amines in near-quantitative (93–98%) yields (Fig. 3).

Mechanistic studies of PSCat method

Luminescence spectra of the reaction components were measured at their representative excesses (conditions B, 10× diluted to ensure **SF** would fully dissolve). While **MFB** showed no change at all after repeated excitations at $\lambda = 375$ nm (Fig. 4A), **SF** underwent a slow photodecomposition over 6–18 min (Fig. 4B; for photodecomposition rates, see ESI†). Upon

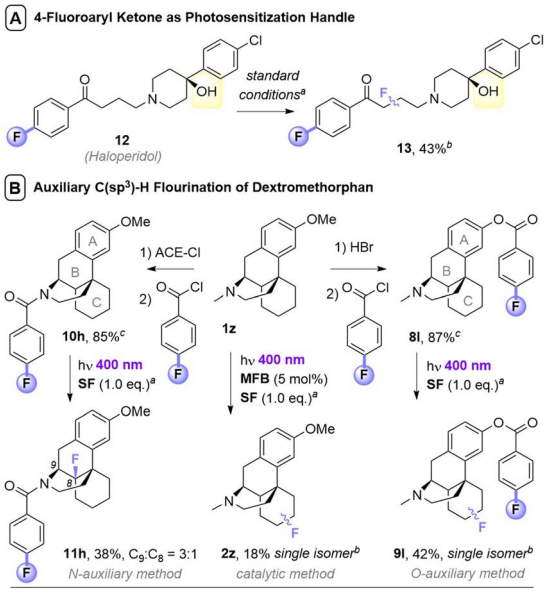

Fig. 2 Applications of photosensitization auxiliary concept. [a]Unless otherwise stated, standard conditions in Table 3B were used, with 1.5 eq. substrate and 1.0 eq. **SF**. Isolated yields given unless stated otherwise. [b]Yield determined by ^{19}F NMR with trifluorotoluene as IS. [c]Overall yields over two steps.

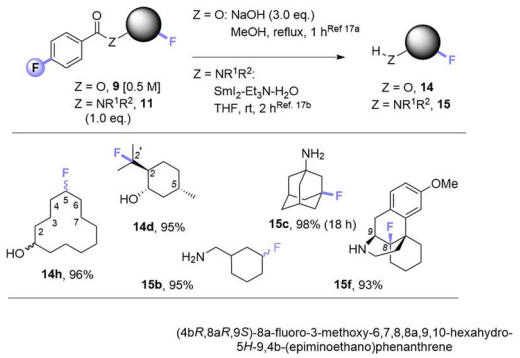

Fig. 3 Cleavage of auxiliaries. Isolated yields are given. See Table 3 for regioselectivity.

mixing **MFB** (12.5 mol% w.r.t. **SF**) with **SF** (8 eq. w.r.t **MFB**), the peak at $\lambda = 434$ nm decreased in intensity by 42% (Fig. 4C). Its shape did not resemble **SF** (no peak at $\lambda = 467$ nm) and even after 5 min of repeated excitations the intensity barely decreased. Lu, Soo, Tan and co-workers also observed that the emission peak shape of **AQN** differed in the presence of **SF**.[9b] Mixing **MFB** with larger excesses of **SF** (Fig. 4C–E) led to buildup of a peak at $\lambda = 467$ nm that more closely resembled **SF**. Interestingly, the presence of **MFB** led to faster photodecomposition of the **SF** peak compared to **SF** alone (Fig. 4, E vs. B). The measured lifetime of **SF** also decreased in the presence of **MFB** (see ESI†). These data corroborate an energy transfer between **MFB** and **SF**, in line with that proposed for previous arylketone catalysts.[9,10] This suggests ^{3}**MFB*** is the excited state involved, and its T_1 energy is well matched with that of **SF**

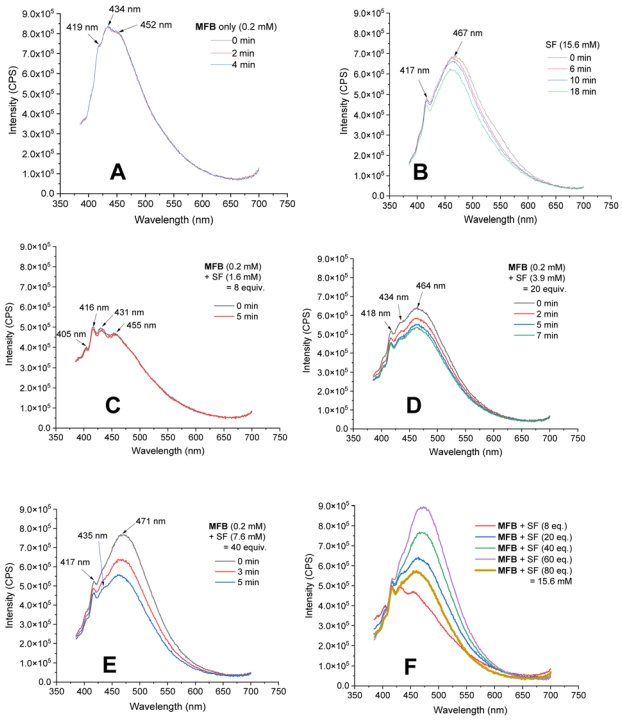

Fig. 4 Luminescence of **MFB** and **SF**. (A) **MFB** only (0.2 mM), repeated measurements. (B) **SF** only (15.6 mM), repeated measurements. (C–E) **MFB** (0.2 mM) with increasing concentrations of **SF**, repeated measurements. (F) **MFB** (0.2 mM) with increasing concentration of **SF**.

(see Table 4, *vide infra*). A radical trapping experiment with 1.5 eq. of TEMPO was performed. As clear evidence of the alkyl chain radical intermediate, a product was detected by LC-MS which matched the TEMPO-bound **16** and no fluorinated product (**2k**) was detected (Fig. 5). Therefore, the mechanism of the **MFB**-catalyzed reaction mirrors that previously proposed and elegantly investigated in the literature for **AQN** (Fig. 6).[9b,12]

Upon photoexcitation and intersystem crossing, ^{3}**MFB*** undergoes E_nT with **SF**. An exciplex is formed involving substrate molecule (**1k**) which facilitates the N–F bond cleavage and HAT process.[9b] Intermolecular HAT occurs between the radical dication of **SF** (**18**) and the most hydridic C(sp^3)–H bond of the substrate (**1k**) that affords the more stable 2° alkyl radical **17** and **SF–H**. Once **17** is generated, fluorine atom transfer (FAT) with **SF** affords **2k**. This may propagate a chain reaction, but a previously reported quantum

Table 4 Triplet energies of reaction components

Entry	Substrate (→ surrogate of)	T_1[a] (kcal mol^{-1})
1	Methyl benzoate (→ **1a**, **1c**)	77.9
2	Benzonitrile (→ **1d**)	76.8
3	Benzamide (→ **1e**)	79.3
4	**MFB**	78.3

[a] Calculated using Time Dependent-Density Functional Theory (see ESI for details).

Fig. 5 Radical trapping reaction of **1k** with TEMPO.

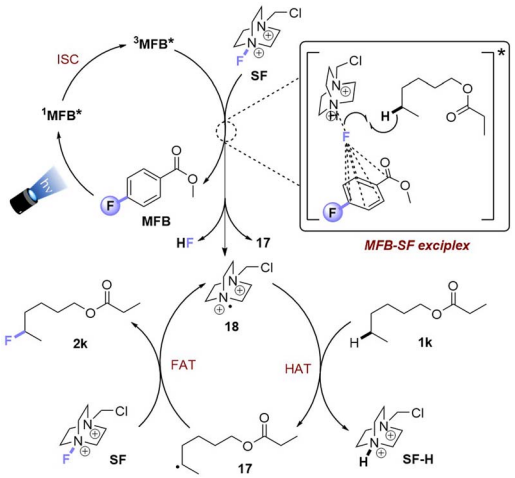

Fig. 6 Proposed reaction mechanism for **PSCat** method.

yield of *ca.* 0.12 seems to oppose this (or suggests an inefficient chain propagation).[9b]

Mechanistic studies of PSAux method

The majority of efforts were directed at understanding (i) the pronounced benefit of the **PSAux** method over the catalytic method, and (ii) the promoting role of the 4-fluorine atom in the **PSAux**. The first observation was that compounds **1c**, **1d** and **1e** all gave no fluorination in the absence of **MFB** (Table 2), despite electronically resembling amyl benzoate (**1a**) and **MFB**. The lack of reactivity of **1e** in the absence of **PSCat** is consistent with the previously reported lack of reactivity of *n*-butylbenzamide (Fig. 1B).[12] The triplet energies (T_1) for directly related compounds are summarized in Table 4. Time-dependent Density Functional Theory (TD-DFT) calculations were used to calculate T_1 for **MFB** (78.3 kcal mol^{-1}, see ESI†). Although the T_1 values for all these compounds[18,19] lay above that reported for **SF** (61.4 kcal mol^{-1}),[9a] no correlation existed between the T_1 values and the efficiencies of the photochemical fluorinations of **1a–1d**, confirming other factors underpinned successful reactivity. To probe further, we examined substrate **5b** for which the catalytic method was ineffective, giving product **21** in only 8% yield (Table 5, entry 1). A control experiment without catalyst (entry 3) revealed this trace reactivity derived from photochemical self-fluorination, akin to amyl benzoate **1a** but in very low efficiency. When a stoichiometric amount (150 mol%) of **MFB** was employed (entry 4), activity of the **PSCat** method was observed, affording product **21** in 47% yield. That the reaction of **8b** without catalyst gave almost double (75%) the yield of **9b** (entry 7) confirmed the **PSAux** provides a beneficial effect beyond simply higher 'effective' catalyst loading. It supports the notion that a preassembly co-locating substrate and **SF** in close proximity sets up a more efficient inner-sphere photochemical process. This is further supported by the fact that the synthetic reactions work equally well under the **PSAux** method without degassing (entry 7 *vs.* 8), but not under the **PSCat** method (entry 4 *vs.* 6) which requires strict freeze/pump/thaw cycling. **NFSI** as a different fluorinating source gave results that were (i) far inferior to **SF** (entries 8 and 9) and (ii) similar with both **PSCat** and **PSAux** methods (see ESI†), suggesting a different, unrelated mechanism operates here. UV-vis spectra of the reaction mixtures of **5b** and **8b** revealed, in both cases, an absorption band at *ca.* 400 nm (Fig. 7, see ESI for details†). This absorption was notably higher than any individual reaction component and was accessible at the synthetic experiments' LED wavelength, suggesting a charge-transfer complex[20] forms between the **PSAux** and **SF**. However, the peak shape and absorption intensity was no different in the case of **5b**'s and **8b**'s reaction mixtures. Given the drastic difference in the efficiency of **5b**'s and **8b**'s reactions, the promoting role of the F atom in the **PSAux**'s clearly does not involve chromophoric changes.

Table 5 Control reactions with different **MFB** loading

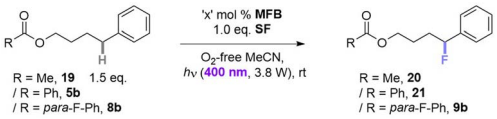

Entry	R (Substrate)	MFB 'x' mol%	Yield[a] (product)
1	Ph (**5b**)	1	8% (**21**)
2	Me (**19**)	1	19% (**20**)
3	Ph (**5b**)	0	10% (**21**)
4	Ph (**5b**)	150	47% (**21**)
5	Me (**19**)	150	30% (**20**)
6	Ph (**5b**)	150[b]	35% (**21**)
7	*para*-F–Ph (**8b**)	0	75% (**9b**)
8	*para*-F–Ph (**8b**)	0[b]	74% (**9b**)
9	*para*-F–Ph (**8b**)	0[c]	23% (**9b**)

[a] NMR yield, based on ^{19}F NMR and trifluorotoluene as IS. [b] Under air. [c] Instead of **SF**, **NFSI** was used as a fluorine source.

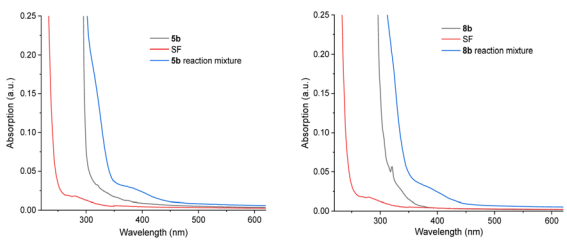

Fig. 7 UV-visible spectroscopy of benzoate esters, **SF** and their reaction mixtures. Left: for benzoate **5b**; right: for 4-fluorobenzoate **8b**.

Given the inability to determine the origin of the promoting effect of the **PSAux**'s F atom by optical spectroscopy, we turned to examine reaction kinetics. The kinetics of **8b**'s reaction were examined by a photoirradiation probe allowing on-line LED irradiation within the NMR spectrometer (see ESI for details†).[21] Consumption of all starting materials and formation of all products could be tracked by time-resolved $^{1}H\{^{19}F\}$ NMR. Samples were compared at the synthetic reaction concentration (0.31 M) to be as representative as possible. **SF** was not fully dissolved under these conditions, meaning unagitated reactions in NMR tubes could not reach yields/conversion rates as high as the synthetic reactions. Nonetheless, this approach was deemed sufficient to observe relative effects. Interestingly, an induction phase was apparent where scarcely any product forms. When repeating the reaction with different amounts of substrate, a clear trend emerged: the induction phase shortened as the loading of **8b** increased. This occurred even in spite of the decreasing (measured) solubility of **SF** as the overall mixture became more non-polar with increasing [**8b**]. While the standard reaction with 1.5 eq. of substrate **8b** had an induction phase of 9.2 h, when 3 eq. **8b** are used it only took 1.9 h until product formation began with a profile typical of a first-order reaction. In summary, by doubling the amount of substrate **8b**, the induction phase can be shortened by 79% (Fig. 8A). The rates of product formation within the linear build-up and the overall yield were, however, independent of substrate loading (Fig. 8B). This may be due to (i) the lack of stirring (an inevitable drawback of *in situ* NMR kinetics), meaning only traces of undissolved **SF** are available for the ongoing reaction, and/or (ii) lower light intensity of the *in situ* irradiation setup (see Table 1, entry 15 *vs.* 17).

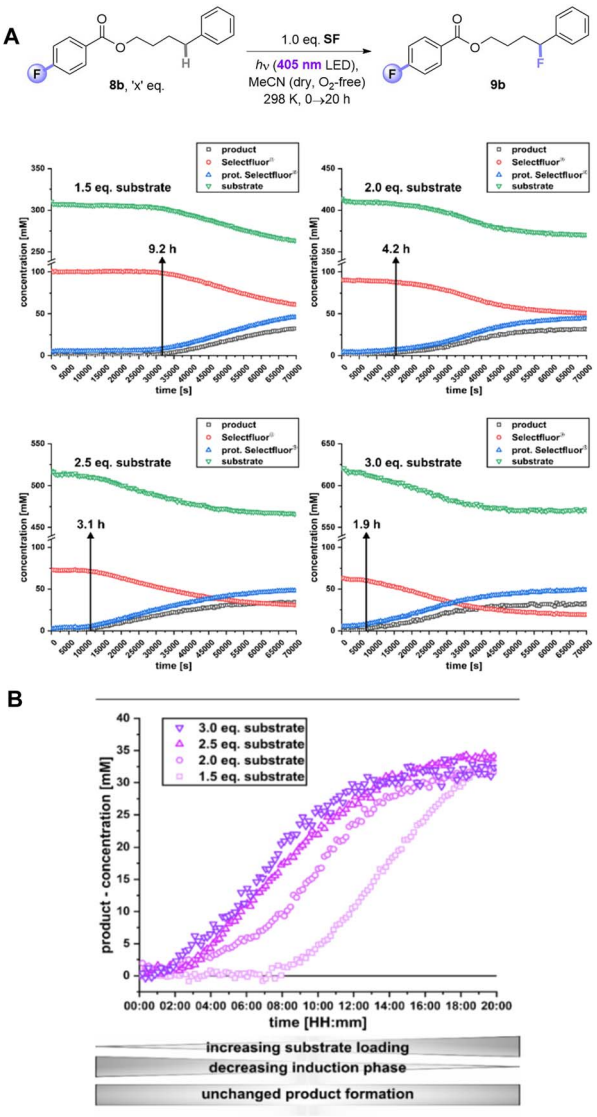

Fig. 8 $^{1}H\{^{19}F\}$ *In situ* illumination NMR reaction monitoring of PSAux. (A) Kinetic profiles of photosensitization auxiliary method with different amounts of **8b**. (B) Detailed comparison of product formation of (**9b**) depending on different substrate loadings.

We hypothesized that a de-aggregation of **SF** may rationalize the induction period. Therefore, Diffusion ordered spectroscopy (DOSY) was performed. The volume of **8b** hardly changed as a function of its concentration (431.4 Å for 0.62 M and 410.1 Å for 0.31 M; Table 6, entries 1 and 2) and was unchanged in the presence of **SF** (entries 4–6). In contrast, the volume of **SF** decreased by 13% from 952.2 Å (entry 3) to 825.3 Å (entry 7) in the presence of 1.5 eq **(8b)** and by 12% to 836.9 Å with 3 eq. **8b** (entry 5) compared to pure **SF** with the same concentration (952.2 Å, entry 3). This confirmed the role of **8b** as a de-aggregation agent. According to the estimated (spherical) molecular volume of **SF** (see ESI†), such a change suggested a change in aggregation from 3 to 2 **SF** molecules. We then examined the size of the **SF** aggregate in the presence of **5b**. The volume of **5b** alone (413.9 Å) was very similar to that of **8b**, consistent with the fact that the fluorine atom is a known bioisostere for H.[6] However, **5b** only de-aggregated **SF** by 4% (entry 9) – a de-aggregating effect 73% smaller than **8b**. Therefore, the F atom in the **PSAux** clearly plays a role in de-aggregating **SF**. This could be explained by a halogen–π interaction as suggested by DFT calculations (see ESI†). However, we note that (i) after this initial de-aggregation with 1.5 eq. **8b**, the volume of components remain unchanged during the reaction and (ii) doubling the concentration of **8b** does not further de-aggregate **SF**. Thus, while de-aggregation of **SF** can explain **8b**'s success *vs.* **5b**'s failure, the substrate concentration benefit on induction period shortening (see Fig. 8) cannot be explained by de-aggregation. Further studies are ongoing in this direction.

Taking together the synthetic benefits of the **PSAux** strategy (handle to direct regioselectivity, remarkable tolerance to O_2, ability to engage molecules with unprotected functionality), our mechanistic studies suggest that the **PSAux** plays two key roles. Firstly, the benzoate **PSAux** engages **SF** in an intimate charge-transfer preassembly (Fig. 9) that absorbs 400 nm (see Fig. 7). The second key role of the **PSAux** is to de-aggregate **SF** (Fig. 9), for which the 4-fluoro atom is especially effective. Moreover, the measured quantum yield of the **PSAux** reaction for **8b** ($\Phi < 0.01$) suggested against a radical chain mechanism. The downstream mechanism then resembles that of the **PSCat** method (Fig. 6) and that proposed in the literature,[9,12] however we propose subsequent steps all occur within the exciplex/solvent cage. E_nT

Table 6 Volumes of different compounds, pure and in reaction, measured by DOSY NMR

Entry	Compound	Composition	c (M)	Average volume[a] with SD (Å^3)
1	**8b**	Pure	0.62	431.4 ± 5.37
2			0.31	410.1 ± 7.44
3	**SF**		0.21[b]	952.2 ± 6.44
4	**8b**	3.0 eq. (**8b**) reaction	0.62	425.6 ± 8.83
5	**SF**		0.21[b]	836.9 ± 17.95
6	**8b**	1.5 eq. (**8b**) reaction	0.31	412.5 ± 6.27
7	**SF**		0.21[b]	825.3 ± 16.40
8	**5b**	1.5 eq. (**5b**) reaction	0.31	413.9 ± 13.24
9	**SF**		0.21[b]	917.5 ± 8.86

[a] Volumes correspond to the mean values of several measurements carried out at different reaction states. For more details see ESI. [b] Weighed in concentration.

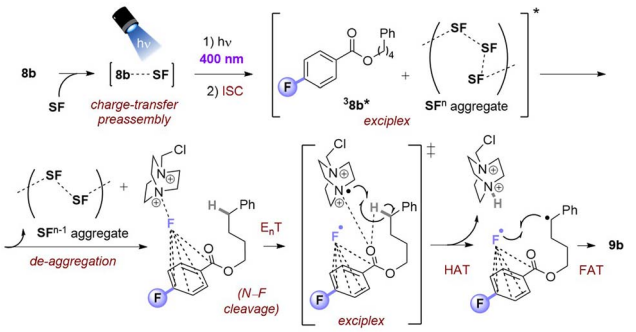

Fig. 9 Proposed reaction mechanism for **PSAux** fluorination by **SF** de-aggregation.

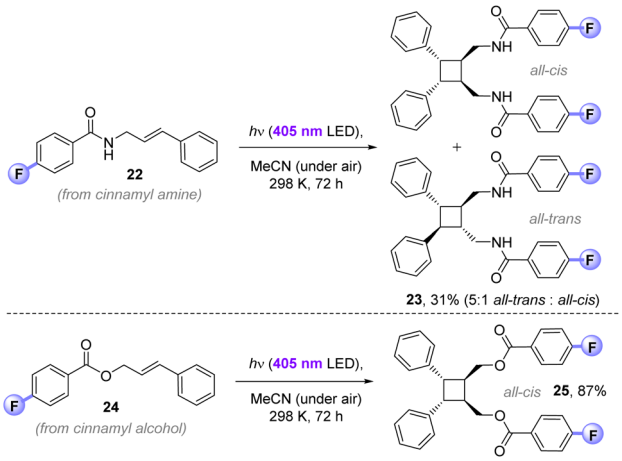

Fig. 10 Application of 4-fluorobenzoyl photosensitizer to [2 + 2]-photocycloadditions.

from ^{3}**MFB*** to **SF** leads to N–F bond cleavage. The benzoate then directs the dication radical to the locally most hydridic C(sp^3)–H bond(s) for HAT that forms a stable (2°, 3°) radical to undergo fluorination. We propose that the beneficial role of de-aggregation is not related to the success of charge-transfer complex formation (see Fig. 7 and the poor reactivity of **5b** *vs.* **8b**), but rather it increases the efficiency of the E_nT step following photoexcitation.

We cannot rule out that the C=O of the ^{3}**PSAux*** engages in photochemical HAT[22] with the C(sp^3)–H bond, but this seems inconsistent with (i) the catalytic lack of reactivities of other *para*-substituted or unsubstituted benzoyl groups (**4b**, **5b**) in **PSCat** or **PSAux** fluorinations and (ii) the clear promotion of **SF**'s photodecomposition as seen in the emission spectra (Fig. 4). The ability to conduct photochemical C(sp^3)–H fluorination reactions in shorter overall reaction times is highly attractive to practitioners, and useful for achieving high yields since **SF** undergoes a competing (photo)decomposition process.

Application of benzoyl auxiliary in other E_nT photochemistry

While the main purpose of our study targeted applications to (and understanding of) C(sp^3)–H fluorinations, we found that the 4-fluorobenzoyl photosensitizer could successfully deliver E_nT [2 + 2]-photocycloadditions *in air*. The 4-fluorobenzamide derivative of cinnamyl amine (**22**) afforded cyclobutane **23** (31%) in exclusive head-to-head regioselectivity, but as a mixture of 'all-*trans*' and 'all-*cis*' diastereomers (5 : 1). In contrast, 4-fluorobenzoylated cinnamyl alcohol **24** underwent [2 + 2]-photocycloaddition to give exclusively the head-to-head, 'all-trans' diastereomer of **25** (87%). The previously reported direct UV excitation of cinnamyl alcohol (10 mM in MeCN, 450 W Hg bulb) affords a 2 : 1 mixture of *cis*-/*trans*-isomers and only traces of the cyclobutane (<5%)[23a] Previously, high yield and selectivity for the cyclobutane was only possible by an iterative (2-step) covalent tethering of two cinnamyl alcohols by di-*iso*-propyldichlorosilane (compared to which, 4-fluorobenzoyl chloride is ~2.5× cheaper) under UV-light and strict degassing.[23] Herein, this is achieved non-covalently, presumably *via* π-stacking of the photoactive 4-fluorobenzoyl motifs under milder visible-light conditions. Where contemporary photocatalytic [2 + 2]-cycloadditions require degassing due to redox or E_nT quenching of the photocatalyst by O_2,[24] the 4-fluorobenzoyl photosensitization auxiliary provides an alternative strategy than can be run *open to air* (Fig. 10).

Conclusions

In conclusion, we report the discovery of a highly efficient visible-light harvesting photosensitizer architecture for the

direct fluorination of unactivated C(sp^3)–H bonds. Our new photosensitizing (4-fluorobenzoyl) group was successfully used both as photosensitizing catalyst and photosensitizing auxiliary. Both catalytic and auxiliary methods were successfully applied to the late-stage functionalization of complex molecules. While a reasonably broad substrate scope of fluorinated products was accessible with catalytic method, the photosensitization auxiliary strategy was found to be far superior in scope and practicality. Substrates that for which the catalytic method was inefficient or ineffective were successfully engaged in higher yields and shorter reaction times, furnishing a general platform for photosensitized fluorination that even tolerates free alcohols/amine functionality and works under air. Mechanistic studies reveal the auxiliary's promoting effects derive from two angles, (i) harnessing **SF** in an intimate charge transfer assembly with **SF** and (ii) in de-aggregating **SF**. The 4-fluorobenzoyl auxiliary allows other E_nT photochemistries to occur in air, where its non-covalent π-stacking interactions alter mechanism and selectivity.

Assemblies between photocatalyst and substrate such as EDA complexes,[20] hydrogen bonding,[22c,d] non-covalent interactions,[25] and ordering of solvent[26] attract ever more attention to uncover the next generation of photocatalytic transformations and provide new frontiers in selectivity and efficiency. This study highlights the emerging importance of how changes in aggregation states of photocatalysts can profoundly influence photochemical reaction mechanisms.[27] Further studies into the structural nature of the charge transfer assembly and the origins of the induction period in photochemical C(sp^3)–H fluorination reactions are ongoing.

Data availability

Experimental and computational data are located in the ESI.†

Author contributions

S. Y. discovered and optimized the photocatalytic and photochemical reaction conditions, synthesized most substrates, synthesized and purified all products, performed synthetic experimental mechanistic studies, measured UV-visible spectra and grew crystals for XRD. W. J. S. conducted all studies on NMR kinetics and DOSY experiments and discovered the induction period and different aggregation states of SF. W. J. S. assisted with 2D NMR structural assignments of complex fluorinated products. X. T. synthesized several substrates and scientifically guided and supervised S. Y. throughout the project. A. S. measured luminescence spectroscopy of SF and MFB. M. J. P. M. performed DFG and TD-DFT calculations and calculated triplet energies. J. P. B. conceptualized the project, guided and supervised S. Y., X. T., M. J. P. M. and A. S. in their contributions. R. M. G. guided and supervised W. J. S., who together wrote the NMR spectroscopic parts of the manuscript and ESI file.† S. Y. and J. P. B. wrote all other sections of the manuscript and ESI file† and addressed peer review additions and corrections. All authors contributed to proofreading the manuscript.

Conflicts of interest

There are no conflicts to declare.

Acknowledgements

S. Y., X. T., and J. P. B. thank the Alexander von Humboldt Foundation for funding, provided within the framework of the Sofja Kovalevskaja Award endowed by the German Federal Ministry of Education and Research. S. Y. is grateful for a DAAD Scholarship and funding provided by the SynCat programme of the Elite Network of Bavaria. S. Y. thanks Julia Märsch and Prof. Robert Wolf and assistance and training on glovebox preparations. R. M. G. and W. J. S. acknowledge financial support by the Deutsche Forschungsgemeinschaft (DFG, German Research Foundation) – 245388561. R. M. G. and J. P. B. are members of DFG TRR 325 'Assembly Controlled Chemical Photocatalysis' (444632635). A. S. was associated to TRR 325 as a Master student at the time of this study. S. Y., J. P. B. and R. M. G. are members of RTG 2620 'Ion Pair Effects in Molecular Reactivity' (426795949). We thank other members of the TRR and RTG for insightful discussions.

Notes and references

1 W. E. Barnette, *J. Am. Chem. Soc.*, 1984, **106**, 452.
2 Selected examples: (*a*) K. L. Hull, W. Q. Anani and M. S. Sanford, *J. Am. Chem. Soc.*, 2006, **128**, 7134; (*b*) E. Lee, A. S. Kamlet, D. C. Powers, C. N. Neumann, G. B. Boursalian, T. Furuya, D. C. Choi, J. M. Hooker and T. Ritter, *Science*, 2011, **334**, 639; (*c*) M. G. Braun and A. G. Doyle, *J. Am. Chem. Soc.*, 2013, **135**, 12990.
3 Selected examples: (*a*) T. Liang, C. N. Neumann and T. Ritter, *Angew. Chem., Int. Ed.*, 2013, **52**, 8214; (*b*) M. Y. Chang, M. F. Lee, C. H. Lin and N. C. Lee, *Tetrahedron Lett.*, 2011, **52**, 826.
4 For selected representative examples, see: (*a*) R. Szpera, D. F. Moseley, L. B. Smith, A. J. Sterling and V. Gouverneur, *Angew. Chem., Int. Ed.*, 2019, **58**, 14824; (*b*) A. Lin, C. B. Huehls and J. Yang, *Org. Chem. Front.*, 2014, **1**, 434; (*c*) M. Rueda-Becerril, C. C. Sazepin, J. C. Leung, T. Okbinoglu, P. Kennepohl, J. F. Paquin and G. M. Sammis, *J. Am. Chem. Soc.*, 2012, **134**, 4026; (*d*) A. Vasilopoulos, D. L. Golden, J. A. Buss and S. S. Stahl, *Org. Lett.*, 2020, **22**, 5753; (*e*) W. Liu, X. Huang, M.-J. Cheng, R. J. Nielsen, W. A. Goddard III and J. T. Groves, *Science*, 2012, **337**, 1322–1325; (*f*) W. Liu, X. Huang, M. S. Placzek, S. W. Krska, P. MqQuade, J. M. Hooker and J. T. Groves, *Chem. Sci.*, 2018, **9**, 1168–1172; (*g*) Y. Zhang, N. A. Fitzpatrick, M. Das, I. P. Bedre, H. G. Yayla, M. S. Lall and P. Z. Musacchio, *Chem. Catal.*, 2022, **2**, 292–308.
5 Selected reviews: (*a*) W. K. Hagmann, *J. Med. Chem.*, 2008, **51**, 4359; (*b*) K. Müller, C. Faeh and F. Diederich, *Science*, 2007, **317**, 1881; (*c*) T. Fujiwara and D. O'Hagan, *J. Fluorine Chem.*, 2014, **167**, 16.

6 S. Yakubov and J. P. Barham, *Beilstein J. Org. Chem.*, 2020, **16**, 2151.

7 Selected examples: (*a*) S. Bloom, C. R. Pitts, D. C. Miller, N. Haselton, M. G. Holl, E. Urheim and T. Lectka, *Angew. Chem. Int. Ed.*, 2012, **51**, 10580; *Angew. Chem.*, 2012, **124**, 10732; (*b*) M. H. Shaw, V. W. Shuftleff, J. A. Terrett, J. D. Cuthbertson and D. W. C. MacMillan, *Science*, 2016, **352**, 1304; (*c*) J. P. Barham, M. P. John and J. A. Murphy, *J. Am. Chem. Soc.*, 2016, **138**, 15482; (*d*) Y. Takahira, M. Chen, Y. Kawamata, P. Mykhailiuk, H. Nakamura, B. K. Peters, S. H. Reisberg, C. Li, L. Chen, T. Hoshikawa, T. Shibuguchi and P. S. Baran, *Synlett*, 2019, **30**, 1178; Selected reviews: (*e*) F. J. A. Troyano, K. Merkens and A. Gómez-Suárez, *Asian J. Org. Chem.*, 2020, **9**, 992; (*f*) J. Kaur and J. P. Barham, *Synthesis*, 2022, **54**, 1461.

8 Selected examples: (*a*) J. B. Xia, C. Zhu and C. Chen, *J. Am. Chem. Soc.*, 2013, **135**, 17494; (*b*) J. B. Xia, C. Zhu and C. Chen, *Chem. Commun.*, 2014, **50**, 11701.

9 Selected examples: (*a*) C. W. Kee, K. F. Chin, M. W. Wong and C. H. Tan, *Chem. Commun.*, 2014, **50**, 8211; (*b*) J. W. Kee, H. Shao, C. W. Kee, Y. Lu, H. S. Soo and C. H. Tan, *Catal. Sci. Technol.*, 2017, **7**, 848.

10 Selected examples: (*a*) D. D. Bume, C. R. Pitts, F. Ghorbani, S. A. Harry, J. N. Capilato, M. A. Siegler and T. Lectka, *Chem. Sci.*, 2017, **8**, 6918; (*b*) D. D. Bume, S. A. Harry, C. R. Pitts and T. Lectka, *J. Org. Chem.*, 2018, **83**, 1565; (*c*) D. D. Bume, C. R. Pitts, R. T. Jokhai and T. Lectka, *Tetrahedron*, 2016, **72**, 6031; (*d*) C. R. Pitts, D. D. Bume, S. A. Harry, M. A. Siegler and T. Lectka, *J. Am. Chem. Soc.*, 2017, **139**, 2208; (*e*) J. N. Capilato, C. R. Pitts, R. Rowshanpour, T. Dudding and T. Lectka, *J. Org. Chem.*, 2020, **85**, 2855; (*f*) During the review of this manuscript, Leckta reported directed fluorinations using endogenous 3° alcohols under O_2-free conditions. 2° alcohols worked only in the presence of inorganic base: S. A. Harry, M. R. Xiang, E. Holt, A. Zhu, F. Ghorbani, D. Patel and T. Lectka, *Chem. Sci.*, 2022, **13**, 7007–7013.

11 S. P. Vincent, M. D. Burkart, C. Y. Tsai, Z. Zhang and C. H. Wong, *J. Org. Chem.*, 1999, **64**, 5264.

12 H. Egami, S. Masuda, Y. Kawato and Y. Hamashima, *Org. Lett.*, 2018, **20**, 1367.

13 Selected examples: (*a*) M. S. Chauhan, G. D. Yadav, F. Hussain and S. Singh, *Catal. Sci. Technol.*, 2014, **4**, 3945; (*b*) P. Sharma and R. K. Sharma, *Chirality*, 2019, **31**, 91.

14 K. Yang, M. Song, A. I. Ali, S. M. Mudassir and H. Ge, *Chem.–Asian J.*, 2020, **15**, 729.

15 N. A. McGrath, M. Brichacek and J. T. Njardarson, *J. Chem. Educ.*, 2010, **87**, 1348.

16 (*a*) D. O'Hagan, *Chem. Soc. Rev.*, 2008, **37**, 308; (*b*) C. Thiehoff, Y. P. Rey and R. Gilmour, *Isr. J. Chem.*, 2016, **57**, 91.

17 (*a*) J. F. Wu, M. M. Liu, S. X. Huang and Y. Wang, *Bioorg. Med. Chem. Lett.*, 2015, **25**, 3251; (*b*) M. Szostak, M. Spain, A. J. Eberhart and D. J. Proctor, *J. Am. Chem. Soc.*, 2014, **136**, 2268.

18 D. R. Arnold, J. R. Bolton, G. E. Palmer and K. V. Prabhu, *Can. J. Chem.*, 1977, **55**, 2728.

19 Y. Kanda, R. Shimada and Y. Takenoshita, *Spectrochim. Acta*, 1963, **19**, 1249.

20 Selected reviews: (*a*) C. G. S. Lima, T. de M. Lima, M. Duarte, I. D. Jurberg and M. W. Paxião, *ACS Catal.*, 2016, **6**, 1389; (*b*) G. E. M. Crisenza, D. Mazzarella and P. Melchiorre, *J. Am. Chem. Soc.*, 2020, **142**, 5461; (*c*) Selected example: during the review of this manuscript, a decarboxylative benzylic fluorination involving a charge transfer complex of SF and DMAP was reported, see: A. Madani, L. Anghileri, M. Heydenreich, H. M. Möller and B. Pieber, *Org. Lett.*, 2022, **24**, 5376–5380.

21 Previous examples of photochemical reaction kinetics: (*a*) K. Chen, N. Berg, R. Gschwind and B. König, *J. Am. Chem. Soc.*, 2017, **139**, 18444; (*b*) H. Bartling, A. Eisenhofer, B. König and R. M. Gschwind, *J. Am. Chem. Soc.*, 2016, **138**, 11860; (*c*) S. Wang, N. Lokesh, J. Hioe, R. M. Gschwind and B. König, *Chem. Sci.*, 2019, **10**, 4580; (*d*) C. Feldmeier, H. Bartling, E. Riedle and R. M. Gschwind, *J. Magn. Reson.*, 2013, **232**, 39.

22 Selected reviews on photochemical HAT using arylketones: (*a*) L. Capaldo and D. Ravelli, *Eur. J. Org. Chem.*, 2017, **2017**, 2056; (*b*) S. Wu, J. Kaur, T. A. Karl, X. Tian and J. P. Barham, *Angew. Chem. Int. Ed.*, 2021, **61**, e202107811; Selected examples: (*c*) N. Berg, S. Bergwinkl, P. Nuernberger, D. Horinek and R. M. Gschwind, *J. Am. Chem. Soc.*, 2021, **143**, 724; (*d*) F. Burg and T. Bach, *J. Org. Chem.*, 2019, **84**, 8815.

23 (*a*) S. A. Fleming and S. C. Ward, *Tetrahedron Lett.*, 1992, **33**, 1013–1016; (*b*) S. C. Ward and S. A. Fleming, *J. Org. Chem.*, 1994, **59**, 6476–6479.

24 Selected examples: (*a*) J. Du and T. P. Yoon, *J. Am. Chem. Soc.*, 2009, **131**, 14604–14605; (*b*) A. Törster, R. Alonso, A. Bauer and T. Bach, *J. Am. Chem. Soc.*, 2016, **138**, 7808–7811; (*c*) D. M. Flores, M. L. Neville and V. A. Schmidt, *Nat. Commun.*, 2022, **13**, 2764.

25 Selected examples: (*a*) S. Wu, J. Žurauskas, M. Domański, P. S. Hitzfeld, V. Butera, D. J. Scott, J. Rehbein, A. Kumar, E. Thyrhaug, J. Hauer and J. P. Barham, *Org. Chem. Front.*, 2021, **8**, 1132; (*b*) X. Tian, T. A. Karl, S. Reiter, S. Yakubov, R. de-Vivie Riedle, B. König and J. P. Barham, *Angew. Chem., Int. Ed.*, 2021, **60**, 20817; (*c*) A. Bhattacharyya, S. De Sarkar and A. Das, *ACS Catal.*, 2021, **11**, 710.

26 Selected examples: (*a*) M. Giedyk, R. Narobe, S. Weiß, D. Touraud, W. Kunz and B. König, *Nat. Catal.*, 2020, **3**, 40; (*b*) J. Kaur, A. Shahin and J. P. Barham, *Org. Lett.*, 2021, **23**, 2002.

27 (*a*) L. Zeng, T. Liu, C. He, D. Shi, F. Zhang and C. Duan, *J. Am. Chem. Soc.*, 2016, **138**, 3958; (*b*) M. J. P. Mandigma, J. Žurauskas, C. I. MacGregor, L. J. Edwards, A. Shahin, L. d'Heureuse, P. Yip, D. J. S. Birch, T. Gruber, J. Heilmann, M. P. John and J. P. Barham, *Chem. Sci.*, 2022, **13**, 1912.